PROGRESS TOWARDS PICOMETER ACCURACY LASER METROLOGY FOR THE SPACE INTERFEROMETRY MISSION

Peter G. HALVERSON, Andreas KUHNERT, Jennifer LOGAN, Martin REGEHR, Stuart SHAKLAN, Robert SPERO, Feng ZHAO,
Tallis CHANG[1],
Edouard SCHMIDTLIN, Roman GUTIERREZ[2],
Thomas R. VANZANDT[3],
Jeffrey YU[4]

California Institute of Technology, Jet Propulsion Laboratory, 4800 Oak Grove Drive, Pasadena, CA 91109. Email: halver@huey.jpl.nasa.gov

[1] Now at Chromux Technologies, Inc. 9255 Deering Ave. Chatsworth, CA 91311. Email: tchang@chromux.com

[2] Now at Siwave Inc., 450 North Brand Blvd. #600, Glendale, CA 91203. Email: e.schmidtlin@siwaveinc.com, r.gutierrez@siwaveinc.com

[3] Now at GEOSense, L.L.C., 115 W. California Blvd. #304, Pasadena, CA 91105. Email: tom.vanzandt@geosense.com

[4] Now at Holoplex Technologies Inc., 600 South Lake Ave, Suite 102, Pasadena, CA 91106. Email: jwyu0@socal.rr.com

ABSTRACT - The Space Interferometry Mission, scheduled for launch in 2008, is an optical stellar interferometer with a 10 meter baseline capable of micro-arcsecond accuracy astrometry. A mission-enabling technology development program is underway at JPL, including the design and test of heterodyne interferometer metrology gauges to monitor the separation of optical components of the stellar interferometer. The gauges are required to have a resolution of 15 picometers and to track the motion of mirrors over several meters. We report laboratory progress in meeting these goals.

1. Introduction

The Space Interferometry Mission[12], a space-borne visible light stellar interferometer with a 10 meter baseline, will be able to measure the angular positions of stars with an accuracy of 5 microarcseconds. To be launched in 2008, its astrometric program includes the search for planets as small as a few earth masses orbiting nearby stars, making accurate parallax distance measurements to stars throughout the galaxy (as far as 25 kpc), measuring the proper motions of stars in nearby spiral galaxies, which will directly yield the distance to the galaxies when combined with existing radial velocity measurements, and measuring MACHO lensing events with sufficient

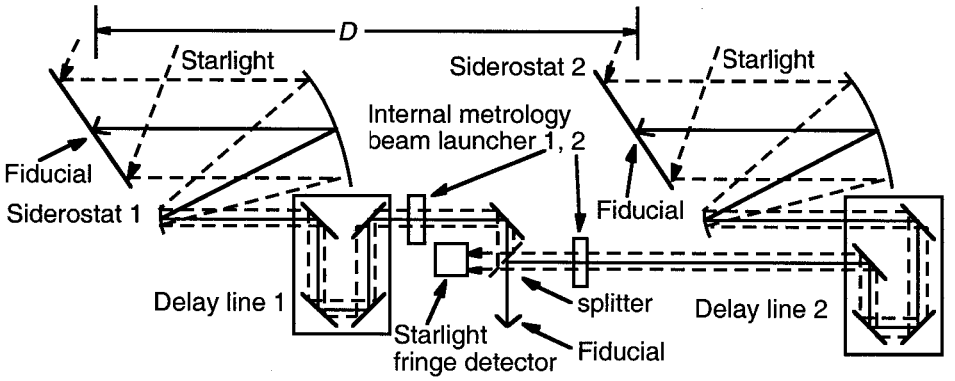

Figure 1: simplified sketch of internal metrology light path (solid line) and starlight (dashed). Internal metrology measures the difference in starlight path(adjusted by the delay lines) required to keep the central starlight fringe locked at the fringe detector. The baseline vector ***D*** is the vector from the center of siderostat 1 to siderostat 2.

accuracy to find the mass of the lensing object.

SIM actually has three interferometers: two to determine the orientation of the spacecraft relative to bright reference stars, while the third, "science" interferometer, makes astrometric observations. (The 7th and 8th siderostats are backups.)

There are two requirements for accurate measurement of the angle between the star and the baseline vector ***D*** that originate at siderostat and ends at siderostat 2 (Fig. 2). The first is that the

measurement of baseline length and the internal path delay must be done to exactly the same point on the telescope. To facilitate this SIM uses fiducials common to both the baseline length measurement system and the internal path length measurement system. The second requirement is that the internal measurement system measures the optical path along the same line of travel as the starlight. In SIM, where metrology gauges are used to measure optical path, it is critical that the metrology gauge beams are launched in a direction parallel to the incoming starlight.

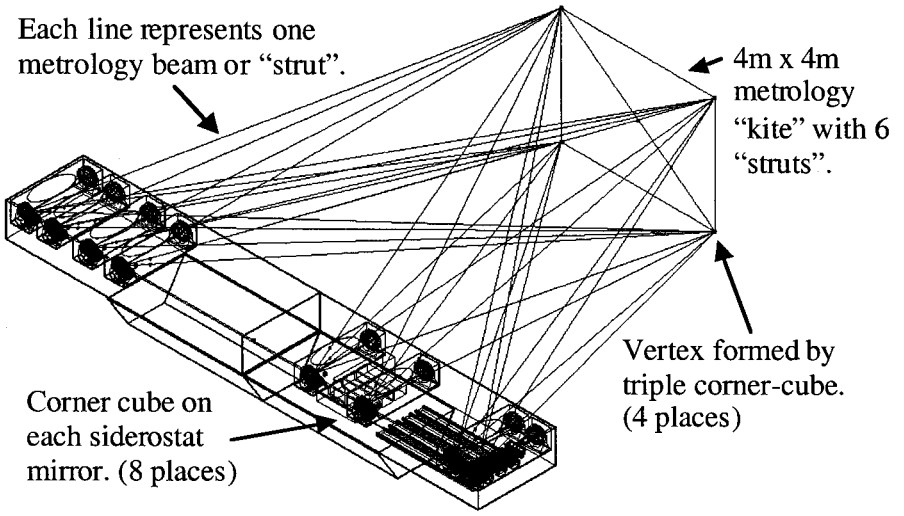

Figure 2: External metrology used to monitor the geometry of SIM to ~100 pm. *Geometry* means the precise lengths, relative directions and positions of $\boldsymbol{D_1}$, $\boldsymbol{D_2}$, $\boldsymbol{D_3}$, the baseline vectors of the three interferometers (science and two reference).

The requirement that the internal metrology travel the same optical path as the starlight, yet not contaminate the starlight fringes, resulted in the choice of 1.3 microns, a wavelength longer than the sensitive range of the starlight detectors.

Measurement of the baseline length could be performed using a single metrology gauge which measures the distance between the fiducials on the siderostats. However, SIM requires the use of three simultaneous interferometers. Given this architectural constraint, the baseline lengths on SIM are measured by creating an external set of fiducials and measuring the positions of the siderostat fiducials using triangulation (Fig. 3).

The α=5 micro-arcsecond = 25 picoradian astrometric accuracy goal for SIM implies knowledge to better than αD =250 picometers of (a) the starlight path length from each siderostat to the beam combiner (splitter) where fringes are formed, and (b) the relative positions of the three interferometers' siderostats.

	Internal metrology requirement	External metrology requirement
Number of gauges	8	42 (kite: 6, roll estimation: 4, siderostats: 32)
Number of gauges for mission success (assuming dispersed failures)	6 (two siderostats are spares)	24 (Kite: 5, roll estimation: 1, siderostat fiducials: 24)
Distance between fiducials	20 meters	Varies: shortest are 4 meters, longest are 12 meters.
Motion; ranges of distances	2.6 meters while changing stars; 10 microns while observing	10 microns
Velocity	2 cm/s while changing stars, 1 micron/sec while observing	
Accuracy (absolute)	Solved for with astrometric data	3 microns rms
Accuracy relative	15 pm rms (1 hour time scale); 8 pm rms (5 minute s)	
Temperature coefficient	2 pm/mK (soak); 50 pm/mK (sensitivity to gradients)	

Table 1: SIM metrology requirements, subject to change as SIM's design evolves.

αD really represents the cumulative uncertainty from a variety of error sources. After a lengthy error budgeting exercise, it was decided that SIM's metrology gauges would have a drift allowance of 15 picometers rms (over several hours), and an absolute accuracy of 3 microns rms. Maintaining these

specifications for the 42 external and 8 internal (including redundant units) metrology gauges for the six year life of the mission has revealed itself to be a challenge.

SIM's metrology specifications are summarized in table 1, the remainder of this paper will discuss the status of efforts to meet these requirements.

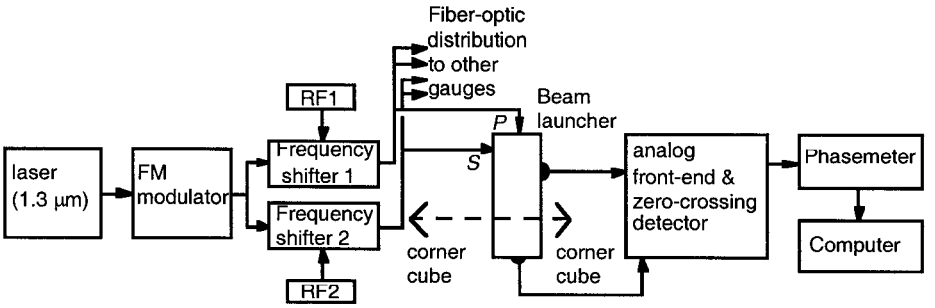

Figure 3: block diagram of metrology system. Building blocks include stable laser source, FM modulator, frequency, fiber-optic distribution system, beamlauncher (with attached photodiodes & preamplifiers, corner cube fiducials, analog front-end & zero-crossing detectors, phasemeters, computers & software. The FM modulator linearly sweeps the optical frequency 84 MHz in a triangle pattern for cyclic averaging. The frequency shifter are fed by RF signals 100 kHz apart to create the 100 kHz heterodyne which will be detected by the photodiodes (attached to beamlauncher).

2. SIM metrology: current design and performance

The metrology system consists of the following building blocks shown in figure 4, and will be described below, except for the laser source, FM modulator and frequency shifters which have been described elsewhere[3] .

Wavelength	1.3 microns
Distance between fiducials	2.5 meters
Beam diameter	5 mm, measured to $1/e^2$ intensity.
Accuracy (absolute)	Not yet measured
Accuracy (relative)	~100 pm (Dominated by polarization leakage. Ignores mispointing, diffraction and thermal error sources)
Temperature coefficient	~100 pm/mK (See text)

Table 2: current performance of metrology prototypes

The overall performance of prototype metrology gauges is summarized in table 2. Thus far, the testing of gauges has been done in air, somewhat limiting our ability to determine the actual relative accuracy. Measured performance is expect to improve with (1) the move to a recently prepared vacuum test chamber and (2) the production of more advanced prototype beamlaunchers.

Beamlaunchers

"Beamlaunchers" refers to the distance measuring interferometer, the optics and photodetectors portion of the metrology gauge (figure 4). Inspired by commercially available devices[4] and further developed at JPL[5], the beamlaunchers use polarizing beam splitters to direct the S-polarized measurement beam to the fiducials and then to a photodiode where it is mixed with a P-polarized, frequency shifted reference beam, yielding the heterodyne signal which contains the desired distance information. The use of two photodiodes allows the suppression of phase perturbations introduced by the optical fibers and laser source: as described later, The distance measurement is derived from the phase *difference* in the two heterodyne signals, hence laser source phase changes (at frequencies much lower than the heterodyne) will be common-mode.

Figure 4b shows an alternate, "racetrack", path for the measurement beam which allows two gauges to measure the distance between the same pair of fiducials. This allows comparison of gauges described later, and offers some advantages, such as passing through fewer optical surfaces.

Although these launchers are of a well-understood design, and described in the references, work is underway to improve them by (1) eliminating stray reflections by introducing small angles to surfaces such as the polarizers, (2) improving the wavefront quality of the beams by careful selection of the optic components and (3) making the path of the reference beam. more similar to the measurement beam by adding a PBS and corner cubes. It is hoped that doing (1) will permit more effective electronic suppression of polarization leakage errors (discussed later), (2) will reduces errors caused by mispointing and (3) will reduce sensitivity to temperature changes.

Finally, a parallel effort is underway to avoid polarization related errors altogether by using spatially separated beams (instead of polarization separated). This will be topic of a future paper.

Corner-cube fiducials

The metrology gauges depend on precise retro-reflectors (corner cubes) to define the endpoints of the distances being measured. Important parameters for this application are dihedral error and planarity of the faces. Because one of internal metrology's endpoints includes the center of the siderostat mirror's front surface (fig. 5a) it is crucial for that corner-cube's vertex to be at the mirror surface. Any residual height of the vertex will have to be accounted for in data analysis, requiring precise knowledge (to ~2 nanometers) of the vertex.

Cornercubes on the kite (fig 5c) are triple cornercubes (TCCs) to accommodate the large fields of view. It is crucial for these to have common vertices to <10 microns to be insensitive to motions of the fiducials.

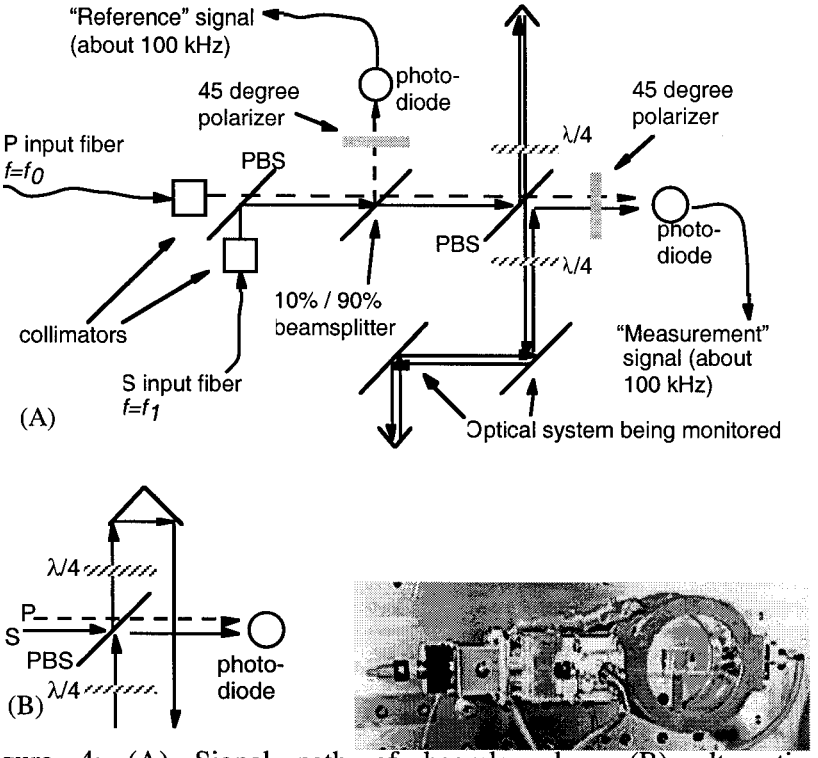

Figure 4: (A) Signal path of beamlauncher. (B) alternative "racetrack" light-path. Photo: P polarized light enters from the left through a polarization maintaining fiber, the reference photodiode is in this middle and the measurement photodiode is at the right. The polarizing beam splitter (PBS) cube, with attached $\lambda/4$ wave plates is visible in the circular housing structure.

To produce various types of cornercubes an assembly technique has been developed using a 6 axis nanopositioning stage and multiple interferometers (HeNe and white light) to assemble prisms (low expansion ULE glass blocs) under real time interferometric monitoring. A low shrinkage UV curing adhesive was preferred over optical contacting. The results are summarized in tables 3 and 4. Recent efforts have demonstrated the ability to assemble corner cubes with dihedral errors as low as 0.1 as, hence for TCC's the dihedral accuracy is limited by the accuracy of the prism angles.

The current TCC design[6] (fig 5b) must be modified slightly to set of 3 pie wedges assembled onto a flat. The assembly technique to produce this geometry and final performance (dihedral, wavefront, non common vertex errors) should be similar to current TCCs.

	Goal	Achieved
Dihedral error	<2 as	<1 as
Planarity of faces	<λ/100 peak/valley (633 nm)	<λ/30 p/v (633 nm)
Vertex-to-siderostat surface distance.	<1 micron	0.8 micron
Vertex-to-siderostat distance calibration	2 nm	~150 nm

Table 3: performance of siderostat fiducials

	Goal	Achieved
Dihedral error	<λ/20 p/v (633 nm) (<1 as)	1 as
Planarity of faces	<λ/20 p/v (633 nm)	<λ/20 p/v (633 nm)
Co-location of corner-cube vertices	<10 microns	2 microns
Vertex co-location calibration	200 nm	Not measured

Table 4: performance of external metrology fiducials (triple corner-cubes).

Analog front-end ("post-amp" electronics)

The output of the beamlaunchers is an analog heterodyne signal (a 100 kHz sinusoid). It is the "post-amp" electronics (figure 6) that convert this to a digital timing signal (a 100 kHz square wave) suitable for the phase measuring electronics.

One might think that the design and fabrication of such a straightforward analog circuit would be easy, but picometer class performance calls for care in preventing distortion of the heterodyne prior

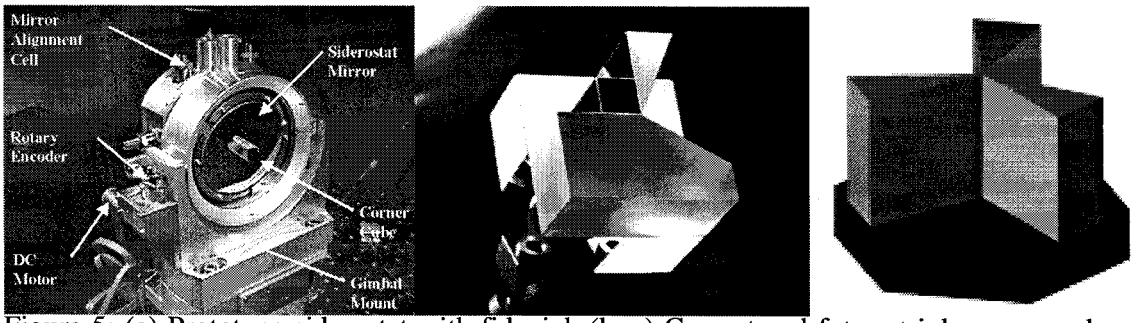

Figure 5: (a) Prototype siderostat with fiducial. (b, c) Current and future triple corner cubes.

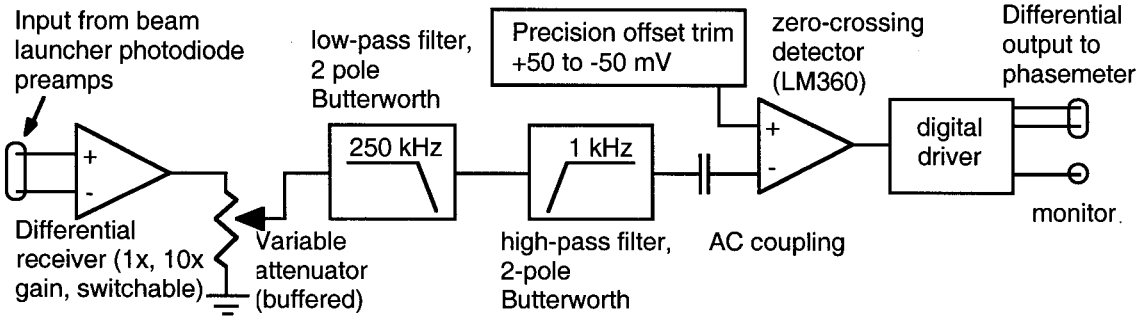

Figure 6: Analog front-end used to convert heterodyne signal to square wave.

to the zero-crossing, avoiding unwanted phase-shifting in the gain and filter stages, ensuring a stable zero-crossing threshold, and decoupling analog and digital circuits. An additional requirement is a high level of AM rejection to prevent variations in metrology beam brightness from being interpreted as phase changes. Signal levels into the post-amps will be affected by variations in laser power, alignment drift, polarization leakage and slewing of delay lines (internal metrology only). Achieved post-amp performance data are summarized in table 5.

No. of channels:	6 (supports 3 metrology gauges.)
Input --> output	100 kHz sine, +/- 10 V FS --> differential TTL
Drift:	1.8 μfringe (1.2 pm) in 6 hours at 100 kHz
Noise:	35 μfringe at 5V into zero-crossing detector. 0.1 μfringe, at 1 sec integration time
A.M. rejection:	1 μfringe (0.65 pm) for 10% amplitude change (balanced common mode). 4 μfringe (2.6 pm) for 10% amplitude change (unbalanced).
Crosstalk:	<0.02 % amplitude artifact observed on one channel, with 5 other channels driven in tandem. (2 pm)

Table 5: Performance of 100 kHz post-amp electronics.

Phasemeter

The heterodyne signals, converted to square-wave by the previously described zero-crossing detectors are fed to the JPL phasemeter board, a VME compatible card that has been described in detail elsewhere[7]. This board measures the phase of the reference photodiode signal relative to the measurement photodiode.

The performance of the phasemeter is summarized in table 6. The instantaneous phase resolution depends on the heterodyne frequency. It can be as good as 1.6×10^{-5} cycles (equivalent to 10 picometers for λ=1.3 microns), at the lowest allowed heterodyne frequency, ~2 kHz. Improved resolution is possible with averaging if random phase noise with amplitude comparable to the instantaneous resolution is present. Tests with a 5 ps resolution digital delay (Stanford Research DG535) have demonstrated accuracy better than 0.8×10^{-4} cycles peak-to-peak with a 100 kHz heterodyne frequency (hence 0.8 ns), using the on-board hardware averaging. Tests over several days using fixed cable delays show a stability of 10^{-5} cycles at 100 kHz (equivalent to 6.5 picometers for λ=1.3 microns), with the temperature staying in a 0.1 °C range.

Number of channels	6
Maximum clock frequency	128 MHz.
Stability	10^{-5} cycles (6.5 pm) for ambient temperature held to 0.1 C.
Range	$2^{32} = 4.3 \times 10^9$ cycles. (2795 meters)
Het. frequency range	1954 Hz to 1.33 MHz
Phase resolution (no averaging)	1.6×10^{-5} cycles (10 pm) at 2 kHz to 0.01 cycles (650 pm) at 1.3 MHz heterodyne frequency. (Improves with averaging)
Velocity range at maximum heterodyne frequency	+/- 0.88×10^6 cycles per second (0.58 meters/second)
Temperature sensitivity	<500 picoseconds/C (32 pm/C)

Table 6. Specifications for the JPL phasemeter. Specifications in picometers assume a 100 kHz heterodyne frequency and 1.3 micron wavelength.

The phasemeter has two averaging modes. In the normal mode, every cycle of the "unknown" input is used in forming averages and the phasemeter is continuously averaging. However certain types of error have a cyclic position dependence[8] that can be nulled by averaging over one cycle of the error[9]. In this scheme, the error is "scanned" by a dithering mechanism synchronized to the phasemeter readout. The phasemeter accommodates this scheme by allowing software to set the start and stop averaging times to correspond to exactly one error cycle, so that overall, the error averages to zero. The efficacy of this "windowed averaging" or "cyclic averaging" will be addressed next.

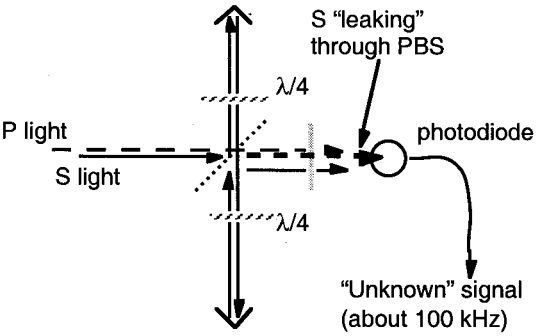

Figure 7: Schematic of polarization leakage problem. A small amount of S polarized light "leaks" through the polarizing beam splitter (diagonal line) and interferes with the S light that makes the round trip between corner cube fiducials. Another leakage term is the small amount of P light that does the round trip (but shouldn't have).

Cyclic averaging

One of the pitfalls of the metrology beam-

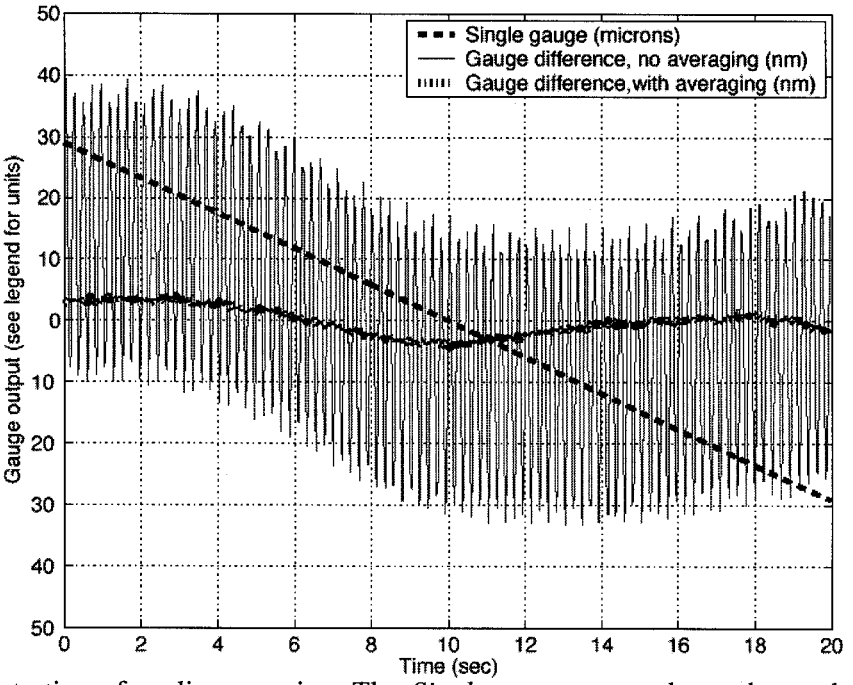

Figure 8: Demonstration of cyclic averaging. The *Single gauge* trace shows the readout of one of the two gauges in response to a 60 micron translation of a common corner cube. The *Gauge difference, no averaging* trace is the difference between two gauge outputs, with cyclic averaging disengaged. The sinusoid is the sum of the periodic nonlinearities of both gauges; its period corresponds to precisely one half-wavelength of corner cube motion, and its amplitude is 20 nm. There is also drift evident in the difference data, attributed to air currents that induce differential fluctuations in the index of refraction seen by the separated beams. The *Gauge difference, with averaging* trace shows the suppression of the periodic error. This trace is from a different 10-second stretch of data, so the drift is not expected to be correlated with the other traces.

launcher designs considered thus far by the SIM program is the systematic error caused by leakage of light through the polarizing beam splitter partly caused by the splitter's finite polarization extinction ratio, and more significantly by the slight miss-polarization of the S or P light incident on the splitter as illustrated in figure 7. To first order, the leakage induces phase shift which advances (or retards) the heterodyne beats ultimately causing a metrology error in L is the inter-fiducial distance we seek to determine: $\text{error}(L) = \lambda\sqrt{P_{\text{leakage}}/P}/4\pi$, where P_{leakage}/P is the fraction of power leaking through the polarizing beam splitter.

Averaging many measurements of L while dithering either L or λ such that $2L/\lambda$ varies by 2π, will in principle remove this error. Figure 8 illustrates this technique. We start with data taken by two metrology gauges. Both gauges are measuring the distance between the same two fiducial corner cubes. One cube is being translated 60 microns in 10 seconds. The difference between the gauges should in principle be zero. Deviations from zero are caused by various misalignments, stray reflections, thermal effects, and the polarization leakage under consideration here. After detrending the difference data, the cyclic error becomes clear: in this case it is 20 nm. To implement cyclic averaging in this system, λ is being modulated by 84 MHz by an AOFM in a 25 Hz triangle pattern which causes $2L/\lambda$ to vary by more than 2π. The phasemeter and software are programmed to search for the averaging time that comes closest to bracketing a 2π variation in $2L/\lambda$ by minimizing the residual cyclic error. The result is a 200 fold reduction in the error, to 100 pm.

Absolute metrology

SIM will be launched in a "folded" configuration, then deployed. This poses a problem for an instrument whose optics are dispersed over 10 meters but whose "absolute" positions must be surveyed to 10 microns. (The 15 picometer specification refers only to knowledge of position *changes* with respect to this absolute starting point.)

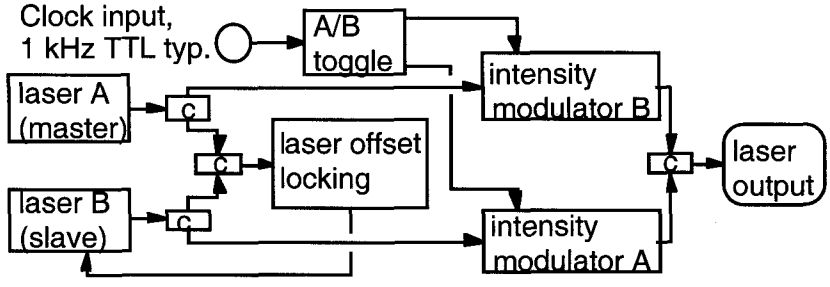

Figure 9: Laser source upgrade for absolute metrology. Light from lasers A and B are held 15 GHz apart by the laser offset locking electronics. A clock signal (the phasemeter readout clock of fig. 0) toggles intensity modulators A and B. The resulting 500 Hz rate, 15 GHz amplitude FM is fed to the metrology gauge for absolute calibration, as described in the text.

The problem to be solved is this: when a given gauge is "turned on", the phasemeter has no way of knowing the integer part of the phase difference between the REF and UNK photodiode signals. The software must be given a starting point after which the phasemeter will continuously "track" changes in phase (until the metrology beam is blocked, or the signal is lost). For internal metrology we can, in principle, move the delay lines to starting points surveyed to a few microns, but for the external metrology such surveying would have to be done after deployment, which is impractical.

Absolute metrology techniques under development at JPL address (1) upgrading existing gauges to give absolute distance information and (2) calibrating the gauges.

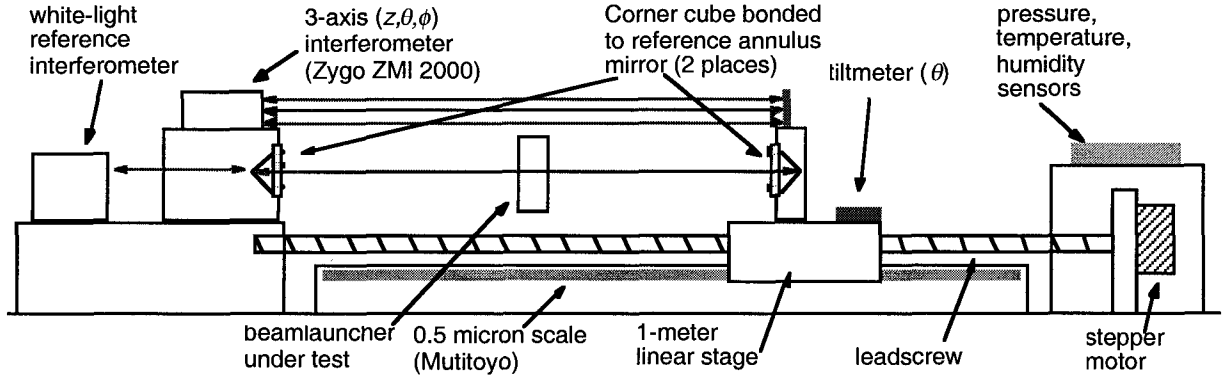

Figure 10: Layout of absolute calibration stand.

Upgrade for absolute metrology

The approach taken at JPL uses the idea that if ϕ, the fractional part of the phase of the metrology beam is measured at two different wavelengths (or frequencies), then it is possible to deduce the absolute distance: $L = \frac{c(N + \phi_2 - \phi_1)}{2(f_2 - f_2)} = \frac{(N + \Delta\phi)c}{2\Delta f}$ where ϕ is in **cycles** and N can be 0, 1, 2... The quantify $c/\Delta f$ is known as the synthetic wavelength and $c/2\Delta f$ represents the wrap-around ambiguity in the measurement. E.g.: in the JPL prototype $c/2\Delta f$=10 cm hence an absolute measurement of 3 cm could mean 3, 13, 23... cm. This is not expected to be a problem in SIM assuming we can trust the initial metrology boom and kite deployment to a few cm. (JEFF: do you agree?)

In practice, the absolute metrology laser source switches frequency at the readout rate of the phasemeter (in the range of 10 to 1000 readouts per second). The switching causes a brief dropout in the heterodyne signals, corrupting the phasemeter integer cycle count. This is not a problem as the integer count will be reset later after the calibration is done. Hence readout of the fractional phase will have ϕ_1 then ϕ_2 then ϕ_1 etc., and from this data L can be derived, to 10 micron accuracy, modulo 10 cm. Next, the frequency switching can be turned off, the phasemeter integer cycle counters reset and the absolute distance information will be available for as long as no loss of heterodyne signals occur. In SIM, it is hoped that this state of accurate absolute metrology knowledge will persist for at least days, hopefully much longer, since the longer the time period between absolute metrology resets with its 10 micron uncertainty, the better the astrometric data can refine the system's calibration.

Calibrating the gauges

The absolute calibration of each metrology gauge beamlauncher will have an uncertain offset caused by delays experienced by the gauge's light as it passes through polarizing beam splitters and quarter wave plates. These are optics whose thicknesses are not tightly controlled in manufacture, hence the offset will be unique for each beamlauncher. The JPL group has constructed a test stand to calibrate various types of beam launchers (fig 10). It is an adjustable and monitored cavity where the launcher to test is inserted and characterized in an absolute sense.

The first step, zeroing the system is done without the beam launcher. The linear stage mounted annulus mirror (with its attached corner cube) is brought into contact with the left annulus. The stage then moves to the right with its motion tracked interferometrically by the Zygo, which also provides information on the stage's deviations from linear travel. During the separation process it is of course vital not to interrupt the beam to maintain fringe count. The launcher is then installed and characterized with the absolute metrology technique described above. The calibration depends on a pre-calibration of the annulus face to corner cube vertex offsets, which has been done with a white-light scanning interferometer. The stage has multiple features for added redundancy and confidence. Contact is sensed both electrically (3 metallic spheres on pads) and optically (white light fringe interferometer sending beams through holes in the annulus). A glass scale is built in the rail providing displacement readout check finally air parameters (mostly temperature) are monitored with a small weather station. From various corroborative tests we have demonstrated that the calibration stage gives absolute measurements good to +/- 1 micron.

Dithering for pointing stability

SIM will be built on a structure that will distort slightly under the influence of thermal changes, torques applied by reaction wheels and the impulse of thrusters during attitude adjustments and

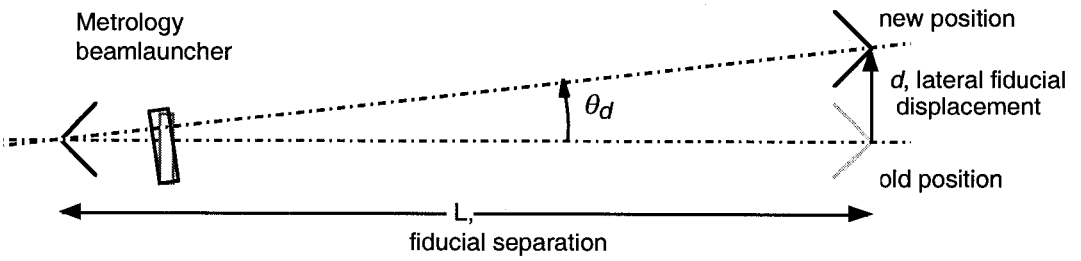

Figure 11: schematic of a disturbance moving a fiducial, requiring a beamlauncher mispointing angle θ_d to maintain alignment.

unloading of angular momentum. Hence the metrology must be able to maintain its accuracy despite lateral motions of corner cube fiducials of a few millimeters. After attitude changes the fiducials are expected to return to their normal positions with a repeatability of 10 microns. In the absence of corrective action, the displacement of a fiducial, sketched in figure 11, will result in an error in the measured length $\Delta L = L\theta_d^2/2 = D^2/2L$. If L=10 m and θ_d > 1.7 microradians, then ΔL > 15 pm, consuming our metrology error budget. To counter this effect, SIM beamlaunchers will rotate in elevation (up/down in the figure) and azimuth (in/out of the paper) to keep the metrology beam parallel to the line connecting the vertices of the corner cubes.

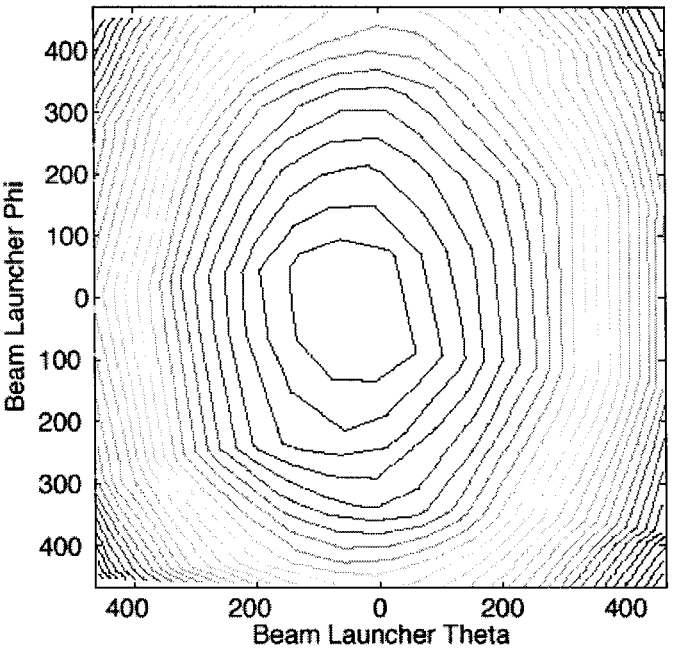

Figure 12: phasemeter output (L) as a function of beamlauncher elevation and azimuth angle. Each contour is 0.002 cycles or 1.3 nm. The central region, near perfect alignment, has a *maximum* in L. $L \approx 2$m. Theta, phi: arbitrary units.

The need to steer the metrology beams calls for the implementation of (1) the ability to sense misalignment and (2) the ability to apply a correction proportional to the degree of misalignment. Reliably sensing the alignment, in two degrees of freedom of the 5 mm diameter metrology beam to a micron relative to the line connecting the corner cube vertices, with conventional detectors such as quad cells, has proven difficult, so a scheme that depends on the error itself has been devised.

Because ΔL is quadratic in θ and ϕ (as seen in figure 12), the sign of the error is not known until a motion reveals its slope. Hence a small (~μradian) sinusoidal *dither* is applied to the beamlauncher's θ and ϕ (at 50 Hz in current tests).

A lock-in amplifier scheme, outlined in figure 13, demodulates the variations in phasemeter output caused by dither. Note that the sinusoidal dithers in θ and ϕ are 90 degree out of phase (causing a circular motion of the beam), to allow independent sensing and control of the two angles.

In our test implementation the metrology data representing L, which is read out at 2 kHz , is

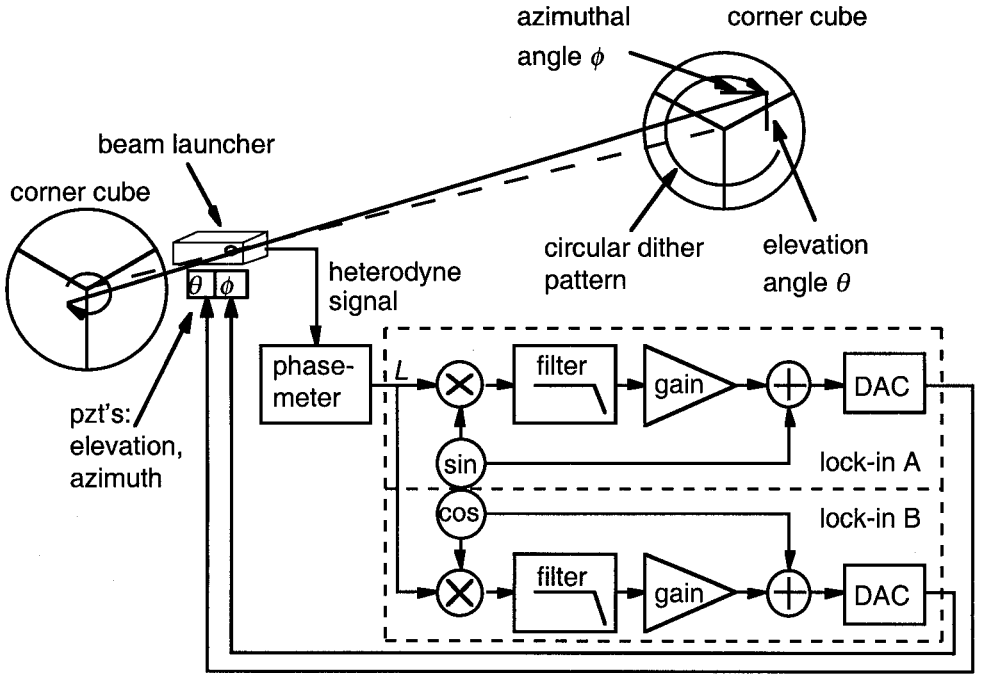

Figure 13: schematic of beam launcher steering in two orthogonal directions θ and ϕ, controlled by dual lock-in amplifiers.

influenced by the deliberate mispointing caused by the dither. The (a) phase and (b) magnitude of changes in the apparent value of *L, at the dither frequency*, indicate the (a) direction and (b) magnitude of the launcher's mispointing, and are fed back to the steering mechanism to restore alignment.

Preliminary tests, such as the data in figure 14 show that this system will respond to lateral displacements of the fiducial (in this case d=110 microns). Limitations of the test setup, due to working in air instead of vacuum, have limited our ability to test this scheme. New tests in vacuum should reveal whether it will meet SIM's requirements.

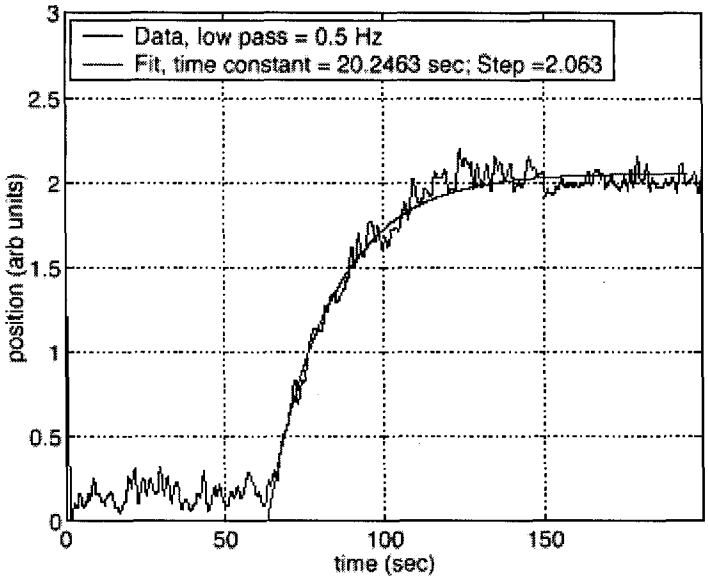

Figure 14: Recovery from a d=110 micron displacement of a corner cube fiducial. L=2 meters. Dither frequency = 50 Hz. Data taken in air.

3. Direction for future work

SIM needs an order of magnitude improvement in metrology gauge accuracy and two orders of magnitude in stability. It is hoped that incremental improvements (adding athermalized reference cavities, improving optics) will close the gap. At the same time, work on non-polarizing beamlaunchers (which will not suffer polarization leakage errors), with improved thermal stability is underway. It remains to be seen which approach will do it first. Progress on absolute metrology has been made. Testing will determine whether the switched frequency technique is sufficiently robust for SIM.

4. Acknowledgments

This research was carried out at the Jet Propulsion Laboratory, California Institute of Technology, under a contract with the National Aeronautics and Space Administration.

---

[1] "The Space Interferometry Mission. Taking Measure of the Universe. Final Report of the SIM Science Working Group", chair Dean Peterson, April 5, 1996. http://sim.jpl.nasa.gov/library/-technical_papers/simswg.pdf

[2] "SIM - Taking the Measure of the Universe", JPL publication 400-811 3/99.

[3] S. Dubovitski, D.J. Seidel, D Liu, R.C. Gutierrez, "Metrology Source for High Resolution Heterodyne Interferometer Laser Gauges", *International Symposium on Astronomical Telescopes and Instrumentation*, SPIE **3350**, pp. 973-984, Kona, Hawaii, 1998.

[4] ZMI 2000 Displacement Measuring Interferometer Systems, Zygo Corp, http://www.zygo.com, HP 10716A High-Resolution Interferometer, Agilent Technologies, http://www.tm.agilent.com

[5] Y.Gürsel, "Laser metrology gauges for OSI", *Proceedings of SPIE conference on Spaceborne Interferometry*, SPIE **1947**, pp. 188-197, 1993.

[6] E.Schmidtlin, "Wide-Angle, Open-Faced Retroreflectors for Optical Metrology", *Photonics Tech Briefs*, **23**, 3, pp. 51a-16a, 3/1999

[7] P.G.Halverson, "A Multichannel Averaging Phasemeter for Picometer Precision Laser Metrology.", *Optical Engineering for Sensing and Nanotechnology (ICOSN '99)*, SPIE **3740**, pp. 646-649, Yokohama, Japan, 1999.

[8] N.Bobroff, "Residual errors in laser interferometry from air turbulence and nonlinearity", *Applied Optics* **26**, 13, 1987.

[9] See Y.Gursel reference.